Fant, Charles

Working Paper

Wind turbine and photovoltaic generating efficiency in Africa

WIDER Working Paper, No. 2016/125

Provided in Cooperation with:
United Nations University (UNU), World Institute for Development Economics Research (WIDER)

Suggested Citation: Fant, Charles (2016) : Wind turbine and photovoltaic generating efficiency in Africa, WIDER Working Paper, No. 2016/125, ISBN 978-92-9256-169-7, The United Nations University World Institute for Development Economics Research (UNU-WIDER), Helsinki, https://doi.org/10.35188/UNU-WIDER/2016/169-7

This Version is available at:
https://hdl.handle.net/10419/161508

UNITED NATIONS UNIVERSITY
UNU-WIDER

WIDER Working Paper 2016/125

Wind turbine and photovoltaic generating efficiency in Africa

Charles Fant*

November 2016

United Nations University World Institute for Development Economics Research
wider.unu.edu

Abstract: As the technology of climate-dependent energy sources is improving—both cheaper and more efficient—the energy sources are becoming more accessible for many of the nations in Africa. However, little is known about the underlying climate that would therefore be harvested by renewable technologies—namely, wind and solar—because these have not been well measured in this region in the past. Here, we present a study that uses publicly available data and methods to develop hourly onshore wind and solar photovoltaic (PV) electricity generation for the years 1979–2010. To do this, we use reanalysis climate data and well-trusted wind farm and solar PV simulation models as well as publicly available geospatial data. The primary purpose of this dataset is to be used in an energy-expansion-planning model of the African continent in a forthcoming study. We find that wind resources vary more over time and space than solar across Africa. Due mostly to these variations in wind resources, we find that the East African Power Pool shows the most potential for wind and solar and the Central African Power Pool shows the least potential. Using an aggregation of areas with the highest potential during the peak demand hours, we develop 'representative sites', one for each country. With these sites, we identify pairs of countries that have potential to participate in mutually beneficial power trade because these resources exhibit negative correlation in reference to each other. Most notably, we find that wind in Kenya and wind in Uganda, which are neighbouring countries, exhibit particularly beneficial characteristics in relation to each other.

Keywords: renewable energy, energy planning, energy trade, Africa
JEL classification: O13, O55, Q42

Acknowledgements: This study of the wind resource in southern Africa was supported by the United Nations University World Institute for Development Economic Research (UNU-WIDER). The author gratefully acknowledges this as well as additional support for this work provided by the MIT Joint Program on the Science and Policy of Global Change through a consortium of industrial sponsors and federal grants.

* Joint Program on the Science and Policy of Global Change, Massachusetts Institute of Technology, Boston, MA, United States; chasfant@mit.edu.

This study has been prepared within the UNU-WIDER project on 'Africa' s energy futures', implemented in collaboration with MIT Joint Program on the Science and Policy of Global Change.

Information and requests: publications@wider.unu.edu

ISSN 1798-7237 ISBN 978-92-9256-169-7

Typescript prepared by Lesley Ellen.

The United Nations University World Institute for Development Economics Research provides economic analysis and policy advice with the aim of promoting sustainable and equitable development. The Institute began operations in 1985 in Helsinki, Finland, as the first research and training centre of the United Nations University. Today it is a unique blend of think tank, research institute, and UN agency—providing a range of services from policy advice to governments as well as freely available original research.

The Institute is funded through income from an endowment fund with additional contributions to its work programme from Denmark, Finland, Sweden, and the United Kingdom.

Katajanokanlaituri 6 B, 00160 Helsinki, Finland

1 Introduction

In general, renewable energy resources are appealing methods to generate power because they do not emit greenhouse gases (GHGs), unlike conventional energy sources. However, the drawback is that they are typically more expensive than the conventional methods. When this is the case, renewable energy only exists as a luxury for wealthy countries that are able to afford the higher upfront costs. However, there is increasing pressure on poorer countries to reduce GHG emissions and many of the governments of these countries continue to promise cleaner energy via renewable energy infrastructure in the not-so-distant future. In fact, one might argue that, if renewable energy is to be the standard in electricity generation in the future, earlier investments in these newer technologies will add valuable experience and help to avoid converting from conventional plants in the near future, especially as renewable energy technology costs decline. Many countries in Africa fit these characteristics, where the existing power sector needs to be scaled up many times larger than the current capacity because of added access, growth in population, and a growing interest in the benefits of modern electronics.

The following study presents an assessment of onshore wind and solar photovoltaic (PV) energy production on the African continent. The primary goal of this study is to develop input data to be used in an electricity capacity expansion model of Africa, described in detail in Rose and Perez-Arriaga (2016). We also hope to produce a dataset that can highlight new and useful characteristics of the wind and solar resources in Africa as individual resources as well as in relation to each other. In brief, our method is to produce hourly, 32-year, power generation time series of onshore wind and solar PV with coverage extending across the continent using publicly available data and methods.

There are other assessments of this kind in the literature. For example, Archer and Jacobsen (2003) assess global wind power potential from observed wind speeds measured at 10m. This is the first attempt to use observed wind speeds to classify mean wind power potential globally. Although Africa is the second-to-lowest continent in wind power potential, Africa, along with Antarctica, are the worst represented continents, and therefore 'should be viewed with caution'. Mentis et al. (2015) map the technical wind energy potential for the continent of Africa using available data and a GIS-based approach. Low-resolution daily wind speed is combined with high-resolution annual mean wind speed using a bilinear interpolation and the Weibull distribution. In addition, various restrictions are applied to better estimate the technical potential, e.g. ground slope, distance to the grid. Although the highest potential lies in the Northern African Power Pool (NAPP), second and third are Southern African Power Pool (SAPP) and East African Power Pool (EAPP), respectively. Interest in renewable energy has grown substantially in South Africa due to increased costs of coal-based power, falling costs of wind and solar, and government involvement (Walwyn and Brent 2015). The costs of wind and PV in South Africa are currently lower than that of coal-fired electricity, a trend which is expected to continue in the future (Walwyn and Brent 2015).

The paper is organized as follows: Section 1 introduces the study; Section 2 presents the data used and methods for estimating onshore wind and solar PV power generation; Section 3 provides an overview of the results; and Section 4 briefly concludes the study with new insights and a way forward.

2 Data and methods

Since measured climate data in this region is sparse and potentially unreliable, a reanalysis dataset is employed. There are many reanalysis datasets publicly available and that have been used in a variety of studies. For this study, the MERRA (Modern-Era Retrospective for Research and Analysis) dataset is used (Rienecker et al. 2011). The advantages of using reanalysis data is that they combine satellite, station, and modelled climate from various sources and generally have been extensively vetted. MERRA is particularly attractive because few reanalysis datasets provide hourly output. MERRA is global and covers the years from 1979 to 2011 (33 years). This dataset has been used in a number of studies on climate-driven electricity generation, e.g. Gunturu and Schlosser (2012) and Fant et al. (2015). With these data, we simulate hourly generating efficiencies defined as the fraction of power generated over the generating capacity. The details of these simulations are described briefly in the following.

2.1 Wind turbine model

Wind speed is estimated using the following logarithmic empirical relationship, taking into consideration roughness length (z0), height (z), and friction velocity (u*) (Stull 1991):

$$V_z = \left(\frac{u_*}{k}\right)\ln\left(\frac{z-d}{z_0}\right) \qquad \text{(EQ-1)}$$

The MERRA data provide the necessary variables for this calculation. In this equation, the wind is assumed to be neutrally stable, a reasonable assumption because at high wind speeds the boundary layer has high wind shear and is therefore approximately neutrally stable.

The spatial scale of MERRA is set to 1/2° by 2/3°, somewhere between mesoscale and synoptic scale, and is hourly. One of the caveats of using data aggregated over a grid is that the aggregation could cause misrepresentations of the climate. Of course, a wind farm would be subject to the wind behaviour at a much smaller spatial scale, so it is important to understand the differences between gridded (i.e. aggregated) and point (i.e. as measured from a station) climate. See Fant et al. (2015) for a full description and analysis of these differences in South Africa where recent wind measurements have been taken using state-of-the-art technology (WASA 2014).

Using the wind speeds estimated from EQ-1 and air density from MERRA, a wind farm model is developed. For simplicity, we have made a number of assumptions with regards to the wind farm technology and layout. This configuration is also used in a study on South Africa (Ummel and Fant 2014), where details are provided. Turbine and array performance are simulated using the wind farm model of Quinlan (1996).

2.2 Photovoltaic model

Climate-dependent solar radiation data necessary for the generation of PV output were also derived from the MERRA dataset. The variables used are Global Horizontal Irradiance (GHI), air pressure at 2 m (Pr), temperature (T), Albedo (α), and wind speed at 2m (V).

First, the parameters related to the sun are estimated. The position of the sun—azimuth (Az) in degrees, actual elevation (El) in degrees and apparent sun elevation (AppEl), which accounts for refraction—is estimated by time, altitude, latitude, longitude, T and Pr using the methods outlined in Hughes (1985). Direct Normal Irradiance (DNI) is estimated using the DISC model

as described in Maxwell (1987), which utilizes GHI, Az, and Pr., and Direct Horizontal Irradiance (DHI) is estimated from GHI and DNI via trigonometry.

The PV model assumes the use of 230W Jinko Solar JKM230M-60B monocrystalline modules in conjunction with SMA Solar SB10000TL inverters. The modules are ground-mounted on single-axis East–West tracking arrays utilizing a backtracking algorithm and maximum rotation of +/-60 degrees. Array spacing assumes a ground cover ratio of 0.4. This configuration is also used in a study on South Africa (Ummel and Fant 2014). Module performance is simulated using the California Energy Commission model and associated module characteristics database (De Soto 2004; Dobos 2012). Temperature correction is provided by the nominal operating cell temperature model of Neises (2011). Inverter performance is simulated using the Sandia National Laboratories model of King et al. (2007) and associated inverter database.

2.3 Geographic exclusions

Certain areas are considered infeasible for construction of PV or onshore wind due to factors that are not captured thus far. These include certain geographic characteristics that are likely to result in infeasible construction or maintenance costs as well as undesirable social costs. In order to exclude these regions, we follow a similar approach as other studies (e.g. Beban 2001; Archer and Jacobsen 2003; Mentis et al. 2015, among others):

1) Steep ground slopes often result in higher construction costs as well as increased wind turbulence that will not be captured in our wind speed estimates. For this reason, we exclude ground slopes greater than 10 per cent using ground slope data from CGIAR-CSI (2006).

2) Water bodies such as oceans, lakes, rivers, and wetlands are excluded. Although wind turbines and solar PV can be constructed on water bodies, we exclude these because of the increased costs, uncertainties of new technologies and construction methods, as well as to avoid interfering with these ecosystems. Water body data is derived from Fischer et al. (2012).

3) Elevation greater than 2000m is excluded because of increased construction costs and thinner air, which is undesirable for wind power. Elevation data is processed from Amante et al. (2009).

4) Urban areas are excluded. For wind, urban areas are not ideal for many reasons. PV, on the other hand, is often constructed on rooftops in urban areas; however, these are typically privately owned small-scale PV and the goal of our study focuses on large-scale utility PV. The urban area database was adapted from the Community Land Model V3.0 input dataset (Oleson et al. 2004).

5) Densely forested areas are also excluded. While building both wind turbines and solar PV at the utility scale is possible in dense forests, the climates are typically undesirable for both: trees cause wind shear and turbulence and forested areas usually occur in places with cloudy/rainy climates with less sunshine. The forest dataset was adapted from Fischer et al. (2012).

6) For simplicity, transmission costs are not directly accounted for in the energy expansion planning model. While conventional power generators can be built near the areas of demand, and therefore remove the need for building excessively long transmission lines, wind and solar are often built in areas where the resource potential is strong, which in

many cases is far from areas of demand. Since we do not have access to demand mapping in Africa, we exclude any areas far from a city. We do this by measuring the MERRA grid centre from cities with current population greater than 50,000 (UN 2015). We restrict this distance to 400km.

Figure 1 shows the areas excluded. Since the distance-to-city exclusion (#6) reduces the area considerably, we show the map with (b) and without (a) this exclusion. In Figure 1a, we see that large areas in central Africa are excluded, largely due to dense forestation, and a large portion of Ethiopia is excluded, largely due to high elevations in the Ethiopian highlands. In Figure 1b, we see that most of the Sahara is excluded as well as portions of Sudan, Angola, and Namibia. Interestingly, the majority of the countries with considerable excluded areas are near to points of large hydropower potential: e.g. the Democratic Republic of Congo and Ethiopia. In these cases, hydroelectric options are likely to be developed before wind or solar options because, although a large upfront investment, they are cheaper in the long term and often dispatchable.

Figure 1: Maps of excluded areas without city distance (a) and with city distance criteria (b)

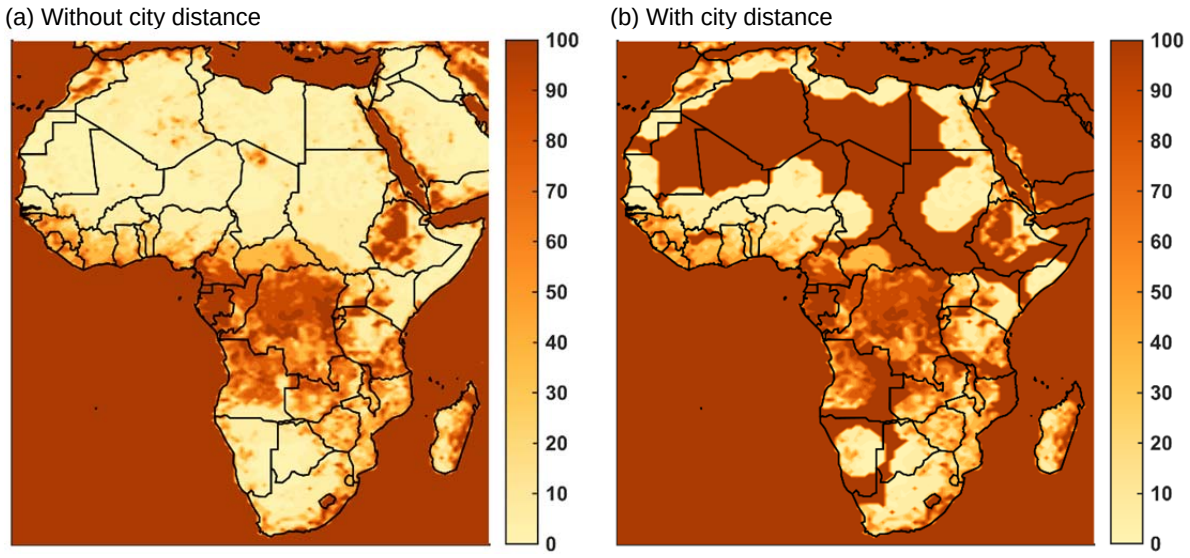

Note: Excluded areas shown as percentage of total, where 100% is completely excluded and 0% is completely included. (a) shows the exclusion without the city distance restriction and (b) shows the exclusion with the city distance restriction.

Source: Author's illustration.

2.4 Time

As is common in energy expansion planning models, representative time slices are used to represent resource availability across time as well as variations in demand. The time slices across the day are:

- **Peak** (17:00–20:00): Period of highest demand
- **Shoulder** (20:00–22:00, 6:00–17:00): Period when moderate demand is expected
- **Off-peak** (22:00–6:00): Period of lowest demand

In order to account for seasonal variations, we also derive the twelve monthly values for each of the time slices reported above. This results in a total of 36 time slices per grid per resource and is described in more detail in Rose and Perez-Arriaga (2016).

Of course, the time slices refer to local time, since they are demand-oriented. We converted to local time using the time zones shown in Figure 2, where the time zone is denoted as annual mean number of hours from Coordinated Universal Time, also known as UTC. Namibia and Morocco both practice daylight saving time, where time zones are shifted by an hour twice a year, and are therefore the only countries not specified by an integer. These time zones may seem like a trivial detail but are important, especially in how well solar resources provide for the peak hours, which are late in the day.

Figure 2: Time zones used, shown as annual mean hours from (UTC)

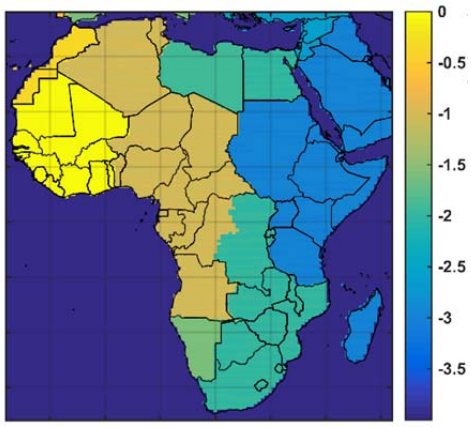

Source: Author's illustration.

2.5 Model regions

The energy expansion planning model groups sub-Saharan African countries into four regional power pools (Table 1). Each country is assigned to a single power pool and island nations are not included. Although not directly related to this particular study, this grouping will be used here to discuss the potential of these countries in particular. Also, the power pool groupings will be important in that countries in the same power pool are more likely to participate in power trade and therefore benefit from interconnection.

Table 1: Grouping of countries into regional power pools

	Southern African Power Pool	East African Power Pool	West African Power Pool	Central African Power Pool
Member countries	Angola Botswana Lesotho Malawi Mozambique Namibia South Africa Swaziland Zambia Zimbabwe	Burundi Djibouti Egypt Eritrea Ethiopia Kenya Rwanda Somalia Sudan[1] Tanzania Uganda	Burkina Faso Cote d'Ivoire Gambia Ghana Guinea Guinea Bissau Liberia Mali Niger Nigeria Senegal Sierra Leone Togo/Benin[2]	Cameroon Central African Republic Chad Congo Democratic Republic of Congo Equatorial Guinea Gabon

Source: Author's illustration.

3 Results

In the following section, we focus on three approaches to describe the behaviour of these wind and solar generation estimates over Africa. In the first, we map the capacity factors of the two resources using means of distinct times, both seasonal and diurnal. Note that in these maps, we show the resources in the excluded regions discussed in 2.3. In the second approach, we plot the resource over each country across the 12 months for each of the time slices, which excludes the regions considered infeasible, using a single calculated 'representative site'. In the third approach, we use the full hourly time series of each representative site to begin to assess the possible benefits of interconnection between countries through power trade, which is often used to mitigate the inherent intermittency typically found in wind power production (e.g. Archer and Jacobsen 2007).

3.1 Resource maps

Figure 3 shows the mean PV generating efficiency for four three-month means—December-January-February (DJF), March-April-May (MAM), June-July-August (JJA), and September-October-November (SON)—and the three diurnal time slices already mentioned. Similarly Figure 4 shows the same maps for wind generating efficiencies. The general pattern is that central Africa and southern West Africa have less potential than northern, eastern, or southern Africa. Not surprisingly, the diurnal pattern is strong: PV is best during shoulder hours, which make up most of the daytime hours, while no potential exists during the off-peak, mostly consisting of night-time, hours. The more interesting maps are those that show the potential during peak hours. Here, we can see patterns from the time zones, where areas on the western edge of the time zone have higher potential than areas on the eastern edge. We also see distinct seasonal patterns in the top two rows, where the southern regions have higher potential in DJF and SON, while the northern regions have higher potential in MAM and JJA.

[1] Sudan and South Sudan are represented as a single country in order to be consistent with most of the available data.

[2] Togo and Benin are also represented as a single country because they share a common utility company and most data group these countries together.

Figure 3: Maps of PV capacity factors for each diurnal time slice—peak, shoulder and off-peak—and four three-month means—DJF, MAM, JJA, and SON.

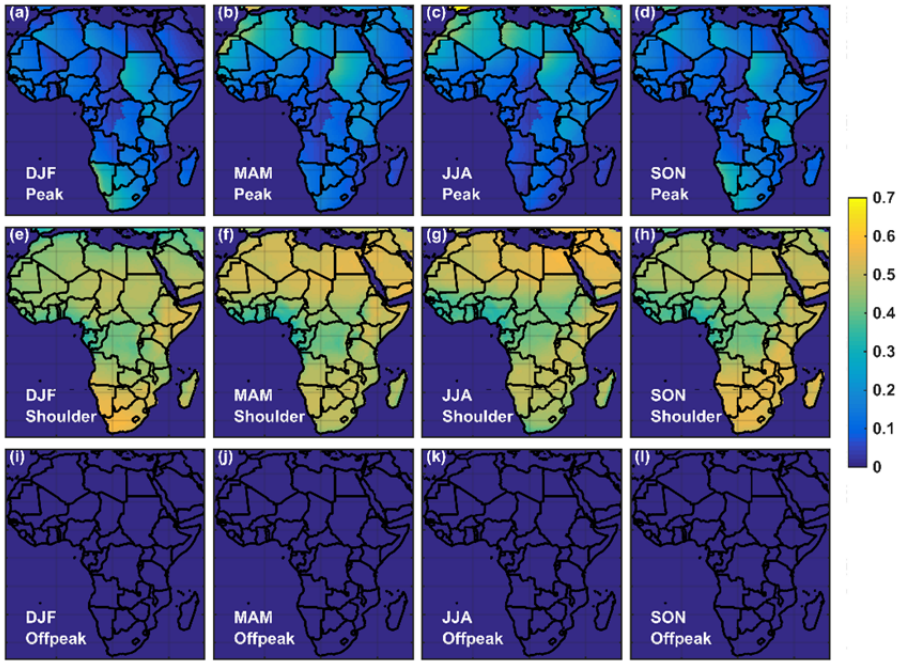

Source: Author's illustration.

Figure 4: Maps of wind capacity factors for each diurnal time slice—peak, shoulder and off-peak—and four three-month means—DJF, MAM, JJA, and SON.

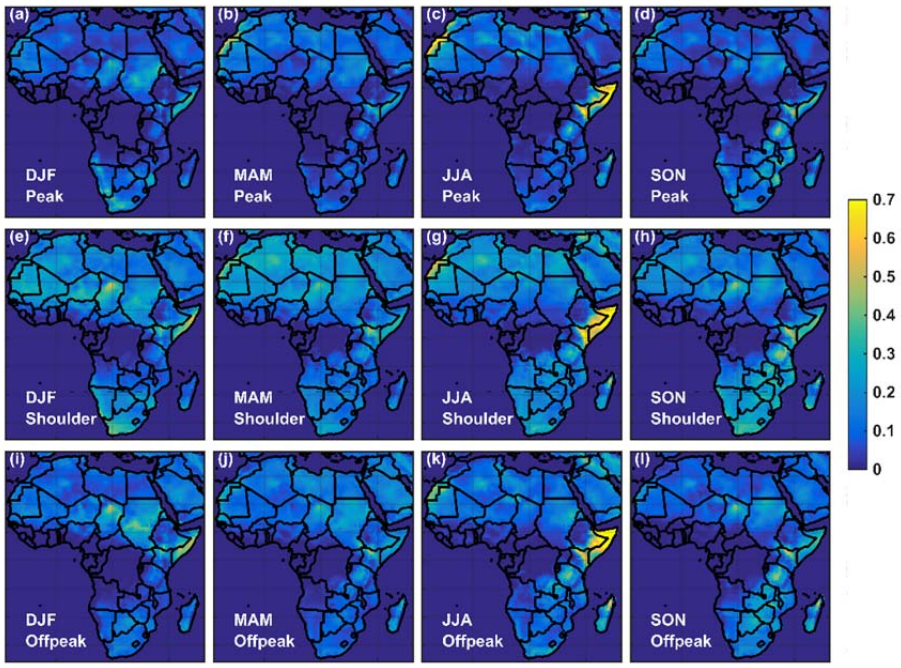

Source: Author's illustration.

Variations in wind power potential are more diverse than solar. In West Africa, most of the potential is in the northwest, in Morocco and western Sahara. This potential would be especially useful during peak hours in MAM and JJA. Other regions of West Africa also show moderate potential up to about 0.4 in parts of Algeria, Mali, Mauritania, and Niger, although these areas tend to be sparsely populated. Wind potential in the southern part of this region has mostly low

potential. Most of central Africa also shows low potential apart from Chad, which shows moderate potential. Southern Africa shows promise for wind power potential, especially during DJF and SON, and during the shoulder period. The most potential is shown in East Africa, especially in Somalia, Ethiopia, Kenya, and, to a lesser degree, Tanzania. However, while the resource is especially strong in JJA, it depletes considerably for the rest of the year.

3.2 Representative sites

Knowing that, if these countries invest in wind and solar power, these investments are likely to be small in proportion to the total generating capacities of the country. In that case, the sites are likely to be placed in areas that provide the most profitable generation. To understand these potentials, we investigate the generating efficiency of a 'representative site' for each country. To determine the power production efficiency of these representative sites, we find the grids within the country that provide the maximum generating efficiencies using the twelve monthly mean values for the peak time slice. In most cases, the same site will provide the highest power potential for multiple months, and, occasionally, a single grid provides the maximum potential for all months. Using these generating potential values from the selected grid/s, we calculate a single generating efficiency ($\bar{E}$) for each country using a weighted mean, accounting for the quality of the generating potential as well as the excluded areas (for partially excluded grids) as follows:

$$\bar{E} = \frac{\sum(E_i A_i C_i)}{\sum A_i C_i} \qquad \text{(EQ-2)}$$

Where E_i is the generating efficiency of each unique grid considered, A_i is the area within the grid feasible for construction and C_i is the number of months for which the grid provides a maximum generating efficiency in the country during the peak hours. This generating efficiency profile is termed the generating efficiency of the 'representative site' and represents the generation of the sites most likely to be utilized in the coming decades. These generating efficiency profiles across the year are shown for the peak time slices (Figure 5), shoulder time slices (Figure 6), and off-peak time slices (Figure 7) for each country considered in the energy-planning model. In these plots, the maximum values are also plotted to show the potential loss of generating efficiency due to multiple sites being averaged and/or the excluded areas. The number of grids is also shown in these plots, which is the total number of unique grids used in the calculation of the single generating efficiency profile.

Figure 5: Seasonal profile of the wind (blue) and solar (red) capacity factors for the representative sites (solid lines) and the maximum capacity factors (dotted line) during peak hours

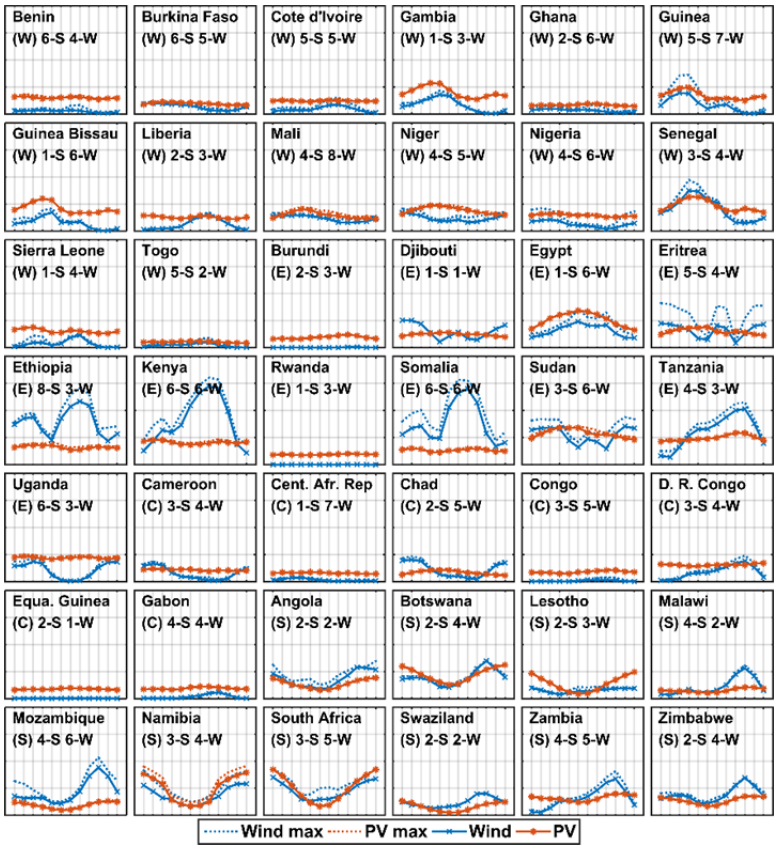

Note: X-axis is the 12 months and Y-axis is 0 to 1. Below the country name is a letter in parenthesis representing the power pool (W=West; E=East; C=Central; S=Southern) and the numbers are the numbers of grids averaged to find the representative best site (S = solar PV and W = wind).

Source: Author's illustration.

For most countries, generating efficiencies are relatively low for both wind and PV resources during peak hours, rarely rising above 0.25 across the year. This is the case for all countries in the Central African Power Pool (CAPP). The only exceptions in the West African Power Pool (WAPP) are Guinea and Senegal, which both show reasonable potential around March-April-May for both wind and PV. For the EAPP, we see countries with the highest potential for wind power, especially in Ethiopia, Kenya, Somalia, and Tanzania. However, these potentials are not consistent across the year with noticeable swings—highest potential from June to September and lowest near the end and beginning of the year—although high potential in Tanzania is slightly later in the year, from August to November. The SAPP also shows potential, for both wind and solar, particularly at the end and beginning of the year, during the warmer months for the region. We see this pattern particularly pronounced in Namibia and South Africa.

As mentioned before, we use a select set of grids to calculate the representative site aggregation. The number of grids in this set is shown in the second line of each plot followed by a dash and a letter: S for solar PV and W for wind. We realize that by aggregating grids, we are making assumptions that may have consequences. Due to transmission costs, the number of grids used would theoretically imply a higher cost to reach the potential shown. Also, since the maximum generating efficiencies are also shown, we can see a portion of the information that is lost, i.e. generating efficiencies reduced, by using the aggregation. For most countries, the maximum and the representative grid values are close, and in many cases they are the same. One exception is Eritrea, where the difference between the maximums and the representative site reach around

0.2 for wind. Since Eritrea is relatively small and stretches along the coast, the representative site algorithm has chosen a number of sites (4 for wind) that have quite different profiles resulting in a much lower aggregate.

Figure 6: Seasonal profile of the wind (blue) and solar (red) capacity factors for the representative sites (solid lines) and the maximum capacity factors (dotted line) during shoulder hours

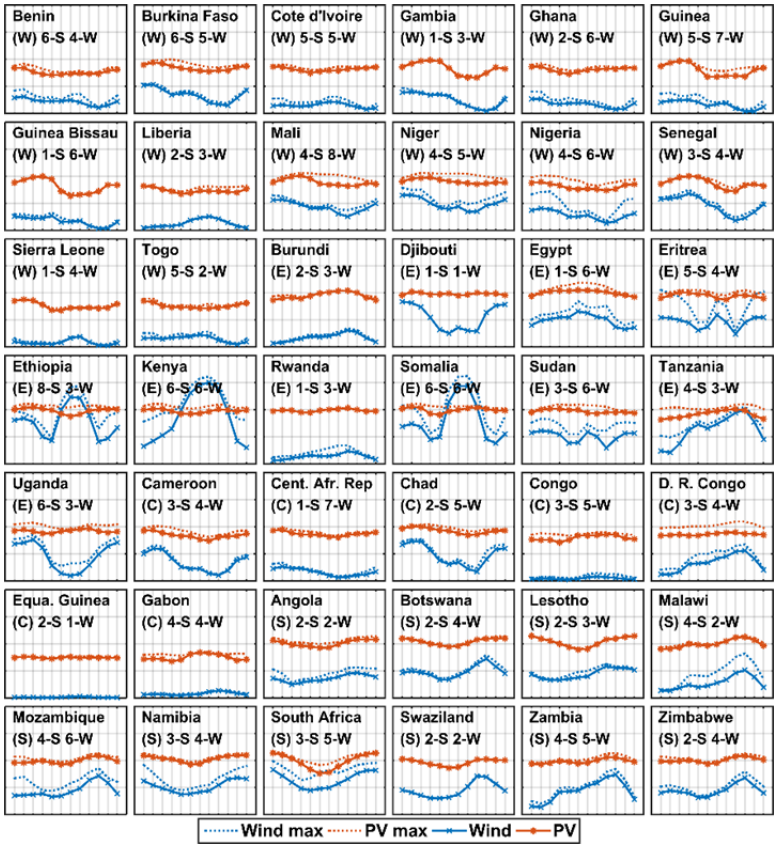

Note: X-axis is the 12 months and Y-axis is 0 to 1. Below the country name is a letter in parenthesis representing the power pool (W=West; E=East; C=Central; S=Southern) and the numbers are the numbers of grids averaged to find the representative best site (S = solar PV and W = wind).

Source: Author's illustration.

The patterns in the wind profiles during peak hours are generally maintained during the shoulder and off-peak hours, especially the more pronounced profile shapes we see in the EAPP. There is a notable difference in the solar PV potential in the shoulder hours, reaching around 0.5 in most countries. As the shoulder hours are during daylight hours, this larger potential is expected. PV potentials are generally higher in the SAPP and EAPP and lowest in the CAPP but not by a considerable amount. Alternatively, PV potential is zero during the off-peak, night-time hours. Wind also has lower potential in most countries during these night-time hours.

Figure 7: Seasonal profile of the wind (blue) and solar (red) capacity factors for the representative sites (solid lines) and the maximum capacity factors (dotted line) during off-peak hours

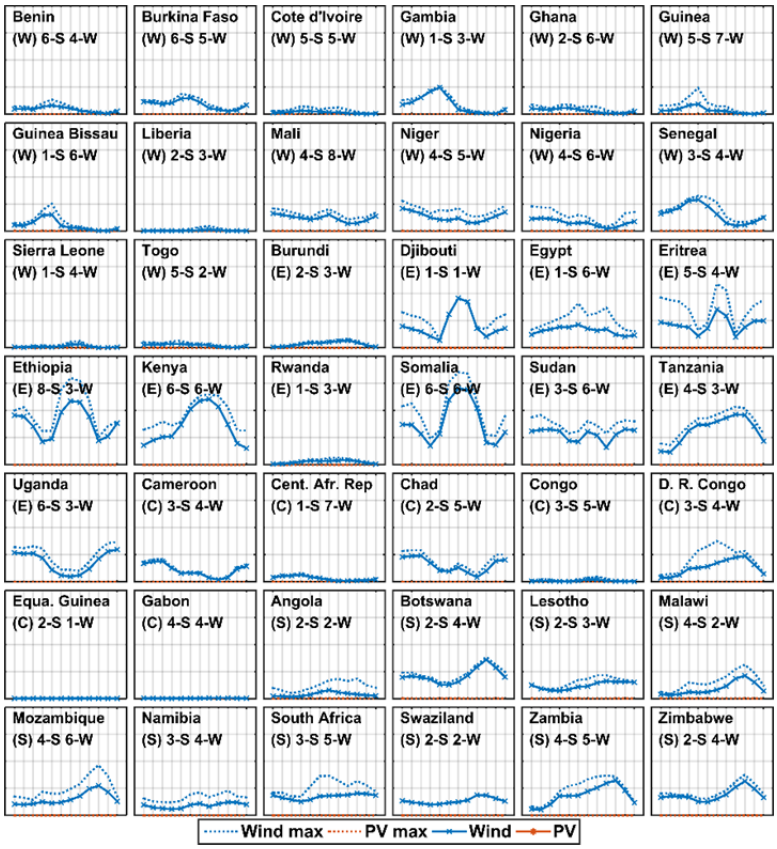

Note: X-axis is the 12 months and Y-axis is 0 to 1. Below the country name is a letter in parenthesis representing the power pool (W=West; E=East; C=Central; S=Southern) and the numbers are the numbers of grids averaged to find the representative best site (S = solar PV and W = wind).

Source: Author's illustration.

3.3 Identifying potential mutually beneficial power trade relationships

In the final visualization of the data, we choose to analyse the hourly data beyond what is used for the energy-planning model, i.e. time slice mean values. Specifically, we are interested in what is lost in using the mean generating efficiencies alone, rather than the full time series, which is too detailed for long-term energy-planning models. To do this, we take all the capacity factors for the best sites in each country and calculate the Spearman rank correlation, R, between each time series using only the peak hours (17:00–20:00). By doing this, we hope to highlight countries that might benefit from energy trade with either wind or solar PV investment. These results are obviously not all-inclusive, since we are only comparing the representative sites. However, since these representative sites are selected to meet demand during peak hours, these investments are likely beneficial in spite of trade benefits and are therefore an added advantage. The results for this are shown in Table 2, where the negative correlation coefficients less than -0.2 are listed. Green shading is used to show those with larger negative correlations and grey shading is used to denote countries that share the same power pool.

Table 2: List of country pairs that share a negative correlation (shown as the correlation coefficient, R) in peak hour wind or solar.

Wind	Wind	R	Wind	Wind	R	Wind	Wind	R
Kenya	Burkina Faso	-0.31	Kenya	Eritrea	-0.24	Sierra Leone	Namibia	-0.21
Liberia	Burkina Faso	-0.32	Liberia	Eritrea	-0.24	Somalia	Namibia	-0.25
Tanzania	Burkina Faso	-0.22	Zambia	Guinea	-0.21	South Africa	Sierra Leone	-0.25
Kenya	Cameroon	-0.33	Namibia	Kenya	-0.35	Uganda	Sierra Leone	-0.24
Liberia	Cameroon	-0.31	South Africa	Kenya	-0.40	South Africa	Somalia	-0.24
Tanzania	Cameroon	-0.20	Uganda	Kenya	-0.42	Uganda	Somalia	-0.22
Kenya	Chad	-0.33	Mali	Liberia	-0.23	Togo	South Africa	-0.23
Liberia	Chad	-0.34	Namibia	Liberia	-0.23			
Somalia	Chad	-0.24	South Africa	Liberia	-0.28	Wind	PV	
Djibouti	Cote d'Ivoire	-0.31	Sierra Leone	Djibouti	-0.34	Liberia	Gambia	-0.22
Uganda	Cote d'Ivoire	-0.24	Somalia	Djibouti	-0.36	Somalia	Gambia	-0.20
Egypt	Djibouti	-0.36	Togo	Djibouti	-0.29	Kenya	Guinea	-0.20
Kenya	Djibouti	-0.54	Namibia	Egypt	-0.26	Liberia	Guinea	-0.25
Liberia	Djibouti	-0.46	South Africa	Egypt	-0.32	Liberia	Guinea Bissau	-0.23
Uganda	Egypt	-0.27	Uganda	Liberia	-0.41			

Note: Green shading is used to denote stronger negative correlations, as this benefit is likely to be stronger. Also, countries in the same power pool are highlighted in grey.

Source: Author's illustration.

There were no instances of PV-to-PV relations with notable negative correlations, five for wind-to-PV, and 37 notable wind-to-wind relationships. Of these that are stronger than -0.4, there are only two that reside in the same power pool: Kenya-to-Djibouti and Uganda-to-Kenya. To illustrate the nature of this kind of relationship, we show a scatter plot of wind generating efficiency in Kenya and Uganda, which are neighbouring countries, in Figure 8, as well as an example time series of year 2000.

Figure 8: Scatter plot of all 32 years, 1979–2010 (left), and time series of one example year, 2000 (right), comparing wind generating efficiencies in Uganda and Kenya during peak hours

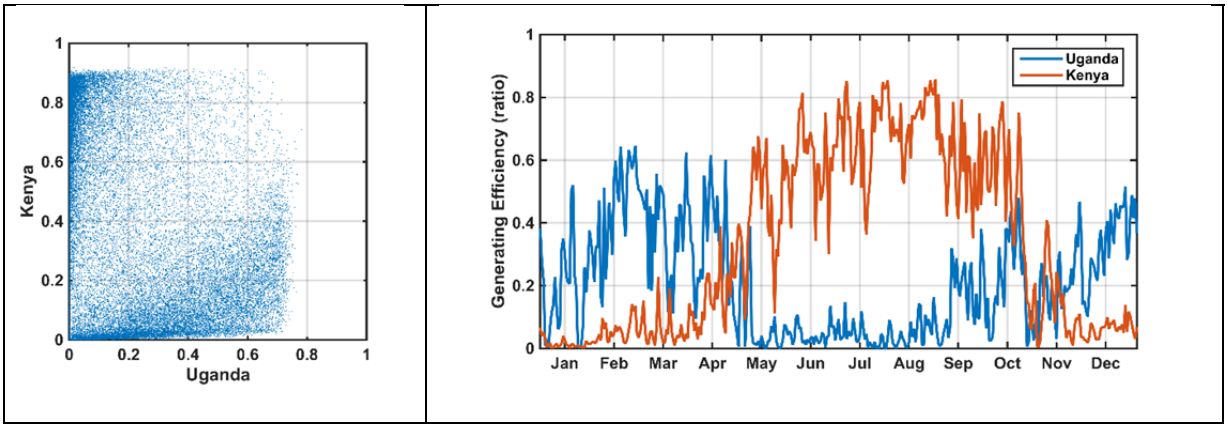

Source: Author's illustration.

In the scatter plot, we can clearly see that when wind power generation is low in Uganda, Kenya has higher generation and vice versa. In the time series plot, we see the same, as well as a clear, out-of-sync annual behaviour in the year 2000, where wind generation is high in Uganda during the beginning and end of the year while wind generation is high in Kenya in May to October, the middle of the year. This kind of analysis can highlight where power trade may be mutually

beneficial between two countries, although more detailed analysis is needed to be sure that this trade potential is robust.

4 Conclusions

We present a straightforward method for producing hourly, multi-year renewable energy performance with publicly available methods and data covering the African continent: a particularly 'data poor' region of the world. We use reanalysis climate data and published methods to predict onshore wind and solar PV power generation. With this, we develop a representative site for each country using an aggregation of the behaviour of area/s with the best potential during peak hours. We then analyse the behaviour of these representative sites, providing the seasonal and diurnal characteristics using statistics often used in energy expansion planning (i.e. means over representative time slices). Finally, we identify relationships between these representative sites that have the potential to be mutually beneficial in mitigating wind or solar intermittency using a measure of correlation.

There are, of course, limitations to this procedure. The most prominent limitation is in the geographic coarseness of the MERRA data grid size, set to 0.5 Latitude by $0.3\overline{3}$ Longitude. In principle, these data represent a mean value across the area of the grid, while wind and solar projects are likely to be much smaller, taking advantage of larger potential at the sub-grid level. This is likely to have a larger effect on the wind power production than the solar since wind is more sensitive to local topography (Fant et al. 2015). There are ways to resolve this statistically (see Ummel and Fant (2014) or Mentis et al. (2015)) and we plan to implement these in the future. Another disadvantage of the presented scheme is in the estimation of diffuse (and thereby direct) radiation from global radiation. We plan to correct this in the future as well by using diffuse radiation derived from satellite measurements. Finally, all generation estimations need to checked and likely calibrated to actual generation output from built plants in the locations they represent. This, however, is impossible until these plants are built; although, corrections can be made on a case-by-case basis as data becomes available from live plants. We also recognize that the characteristics of the specific wind farm and solar PV technologies and configurations impact the results. In the future, we plan to implement alternatives to those presented here for comparison.

With these caveats in mind, we focus our conclusions on big picture characterizations that are more qualitative in nature by identifying patterns and comparing the regions or countries with each other, rather than implying a more technical assessment of the wind and solar resources. We find that of the four power pools, the most resource-rich is the EAPP, largely due to high wind potential, which varies across regions more substantially than solar. The power pool with the least wind or solar resource is the CAPP, although it should be noted that the CAPP has the highest hydropower potential of the power pools due largely to the planned Inga projects on the Congo River. The SAPP also shows relatively high potential, although the potential tends to vary through the year, often with both wind and solar low during colder months. For solar PV, we find that during peak hours, the location in relation to the time zone has a substantial effect, with higher potential for locations on the western edge of the time zone. These regions are able to take advantage of the evening sun more efficiently. As the time zone is typically determined by the government, and can be altered, one can imagine policies to shift time zones in order to make solar energy more effective during the peak. Finally, we find that there are a number of country pairs that exhibit noticeable negative correlations in relation to each other during peak hours. These relationships may highlight the potential of a mutually beneficial power trade if both choose to build the infrastructure, which is likely to be much cheaper than running quick-

start backup generators when power is not being produced. This is especially true for countries close to each other, e.g. wind in Uganda and Kenya.

In forthcoming studies, we plan to improve on the generated data, as mentioned. We also plan to further explore the characteristics of wind and solar power in Africa with more advanced statistical methods like Principal Component Analysis to better understand interconnection benefits (e.g. Fant et al. (2015)) or Spectral Analysis to understand common cycles in the data. We also plan to assess effects of multi-year climate phenomena like the El Nino Southern Oscillation or shorter, intra-annual phenomena like the Madden-Julian Oscillation as well as possible changes in the long-term mean due to climate change, as done in Fant et al. (2016).

References

Amante, C., and B.W. Eakins (2009). 'ETOPO1 1 Arc-Minute Global Relief Model: Procedures, Data Sources and Analysis'. NOAA Technical Memorandum NESDIS NGDC-24. National Geophysical Data Center, NOAA. http://doi.org/10.7289/V5C8276M (accessed on 10 October 2015).

Archer, C.L., and M.Z. Jacobson (2003). 'Spatial and Temporal Distributions of US Winds and Wind Power at 80 M Derived from Measurements'. *Journal of Geophysical Research*, 108: 42–89.

Archer, C.L., and M.Z. Jacobson (2007). 'Supplying Baseload Power and Reducing Transmission Requirements by Interconnecting Wind Farms'. *Journal of Applied Meteorology and Climatology*, 46: 1701–17.

Baban, S.M., and T. Parry (2001). 'Developing and Applying a GIS-assisted Approach to Locating Wind Farms in the UK'. *Renewable Energy*, 24(1): 59–71. Available at: http://doi.org/10.1016/S0960-1481(00)00169-5 (accessed on 12 November 2015).

CGIAR-CSI (2006). 'NASA Shuttle Radar Topographic Mission (SRTM)'. The SRTM data is available as 3 arc second (approx. 90m resolution) DEMs. Available at: http://srtm.csi.cgiar.org/ (accessed on 11 September 2015).

De Soto, W.L. (2004). 'Improvement and Validation of a Model for Photovoltaic Array Performance'. M.S. Thesis, University of Wisconsin-Madison.

Dobos, A.P. (2012). 'An Improved Coefficient Calculator for the California Energy Commission 6 Parameter Photovoltaic Module Model'. *Journal of Solar Energy Engineering*, 134(2).

Fant, C, U.B. Gunturu, and C.A. Schlosser (2015). 'Characterizing Wind Power Resource Reliability in Southern Africa'. *Applied Energy,* 161: 565–73. Available at: http://doi:10.1016/j.apenergy.2015.08.069 (accessed on 20 May 2015).

Fant, C, C.A. Schlosser, and K. Strzepek (2016). 'The Impact of Climate Change on Wind and Solar Resources in Southern Africa'. Applied Energy. http://doi:10.1016/j.apenergy.2015.03.042 (accessed on12 November 2015).

Fischer, G., F.O. Nachtergaele, S. Prieler, E. Teixeira, G. Toth, H. van Velthuizen, L. Verelst, and D.A. Wiberg (2012). 'Global Agro-Ecological Zones, Model Documentation'. IIASA and FAO. Available at: http://www.iiasa.ac.at/Research/LUC/GAEZv3.0/docs/GAEZ Model Documentation.pdf (accessed on 3 July 2015).

Gunturu, U.B., and C.A. Schlosser (2012). 'Characterization of Wind Power Resource in the United States'. *Atmospheric Chemistry and Physics Discussions,* 12(20). http://doi:10.5194/acp-12-9687-2012 (accessed on 3 May 2015).

Hughes, G. (1985). 'Grover Hughes' Class and Related Class Materials on Engineering Astronomy at Sandia National Laboratories'. Albuquerque, New Mexico: Sandia National Laboratories.

King, D.L., S. Gonzalez, G.M. Galbraith, and W.E. Boyson (2007). *Performance Model for Grid-connected Photovoltaic Inverters*. Albuquerque, New Mexico: Sandia National Laboratories.

Maxwell, E.L. (1987). 'A Quasi-Physical Model for Converting Hourly Global Horizontal to Direct Normal Insolation'. Technical Report No. SERI/TR-215-3087. Golden, CO: Solar Energy Research Institute.

Mentis, D., S. Hermann, M. Howells, M. Welsch, and S.H. Siyal (2015). 'Assessing the Technical Wind Energy Potential in Africa: A GIS-based Approach'. *Renewable Energy*, 83: 110–125. Available at: http://doi.org/10.1016/j.renene.2015.03.072 (accessed on 15 November 2015).

Neises, T. (2011). 'Development and Validation of a Model to Predict the Cell Temperature of a Photovoltaic Cell'. M.S. Thesis, University of Wisconsin-Madison.

Oleson, K.W., Y. Dai, G.B. Bonan, R.E. Dickinson, P.A. Dirmeyer, F. Hoffman, P. Houser, S. Levis, G.-Y. Niu, P.E. Thornton, M. Vertenstein, Z.-L. Yang, and X. Zeng (2004). 'Technical Description of the Community Land Model (CLM)'. National Center for Atmospheric Research May, 186 p. Available at: http://www.cgd.ucar.edu/tss/clm/distribution/clm3. 0/TechNote/CLM Tech Note.pdf (accessed on 15 November 2015).

Quinlan, P.J.A. (1996). 'Time Series Modeling of Hybrid Wind Photovoltaic Diesel Power Systems'. M.S. Thesis, University of Wisconsin-Madison.

Rienecker, M.M., M.J. Suarez, R. Gelaro, R. Todling, J. Bacmeister, E. Liu, M.G. Bosilovich, S.D. Schubert, L. Takacs, G.-K. Kim, S. Bloom, J. Chen, D. Collins, A. Conaty, A. da Silva, W. Gu, J. Joiner, R.D. Koster, R. Lucchesi, A. Molod, T. Owens, S. Pawson, P. Pegion, C.R. Redder, R. Reichle, F.R. Robertson, A.G. Ruddick, M. Sienkiewicz, and J. Woollen (2011). 'MERRA: NASA's Modern-Era Retrospective Analysis for Research and Applications'. *Journal of Climate Change*, 24(14): 3624–48.

Rose, A., and I. Perez-Arriaga (2016). 'Technical Note: Proposed Model for Regional Power Sector Integration in Africa'. WIDER Working Paper 2016/125. Helsinki: UNU-WIDER.

Stull, R.B. (1991). *An Introduction to Boundary Layer Meteorology, Volume 13*. First edition. Dodrecht: Kluwer Academic Publishers.

Ummel, K, and C. Fant (2014) 'Planning for Large-Scale Wind and Solar Power in South Africa'. UNU-WIDER Working Paper 121/2014 Helsinki: UNU-WIDER.

United Nations (2015). *World Urbanization Prospects: The 2014 Revision.* (ST/ESA/SER.A/366) Department of Economic and Social Affairs, Population Division. New York, NY: United Nations.

Walwyn, D.R., and A.C. Brent, (2015). 'Renewable Energy Gathers Steam in South Africa'. *Renewable and Sustainable Energy Reviews*, 41: 390–401. Available at: http://doi.org/10.1016/j.rser.2014.08.049 (accessed on 5 December 2015).

WASA (Wind Atlas for South Africa) (2014). Available at: http://www.wasaproject.info (accessed on 21 August 2015).